Optimizing Alzheimer's Disease Detection: An Enhanced Approach Weight-based Beetle Swarm Optimization with SVM

Eman M. Ali
Department of Scientific Computing, Faculty of Computers and Artificial Intelligence, Benha University, Benha, Egypt

Mohamed A. Mahfouz
Department of Information System, Integrated Thebes Academy for Science, Giza, Egypt

Howida Y Abd ElNaby
Department of Computer Science, Faculty of Computers and Artificial Intelligence, Fayoum University, Fayoum, Egypt

ABSTRACT
It is essential for radiologists to identify Alzheimer's disease early to ensure accurate diagnosis and access to treatment. Medical imaging, such as Magnetic Resonance Imaging (MRI), are becoming increasingly difficult to diagnose. This study sought to develop a hybrid framework to use MRI scans to detect Alzheimer's disease. The suggested approach entails applying adaptive median filtering as a pre-processing step to MRI scans, extracting features based on hybrid wavelet partial Hadamard transform (hybrid WPHT) and discrete local binary pattern (DLBP). The next step in the feature selection process is to reduce the dimensionality of the features using the adaptive Harris-Hawk optimization (AHHO) approach. This greatly enhances the performance of the classifier by further refining its parameters using the Improved Weight-Based Beetle Swarm algorithm (IW-BS) and the Optimized Support Vector Machine (OSVM) classification. The MRI image classifies as Mild, Very Mild, or Normal. The results of the study demonstrate that this proposed methodology is more accurate, precision, and recall, specificity, F-score, running time, under the curve (AUC), and receiver operating characteristics (ROC)

Keywords
Magnetic Resonance Imaging, Optimal Support Vector Machine, Hyper-Parameter Tuning, Feature Extraction, Kernel Parameter, Hybrid Wavelet.

1. INTRODUCTION
As the world's population ages, the incidence of Alzheimer's disease (AD) has reached an epidemic level, presenting several challenges to healthcare systems around the world. Alzheimer's disease is a progressive form of neurodegeneration, which is characterized by cognitive impairment, memory decline, and a variety of behavioural and functional dysfunctions [1]. The effective treatment of AD, the execution of interventions, and the assessment of prospective therapeutic regimens all depend on an accurate and prompt diagnosis. Because magnetic resonance imaging (MRI) is non-invasive, highly spatialized, and able to provide information on both structural and functional abnormalities in the brain associated with AD, it has become an increasingly significant diagnostic tool in the endeavour to diagnose AD early [2]. The complex pathophysiological mechanisms that lead to the development of Alzheimer's disease (AD), including the buildup of plaques and tangles of tau proteins, result in neurodegeneration and the degeneration of the brain. These alterations can be observed through a variety of imaging techniques, and MRI provides a comprehensive overview of the structural changes in the brain over time. MRI-based imaging techniques have become increasingly important in Alzheimer's disease research and providing insight into the progression of the disease and enabling the development of new diagnostic techniques and therapeutic objectives [3].

Recent advances in the detection of Alzheimer's disease using MRI, as well as the techniques and approaches developed to improve sensitivity and specificity, are explored. Current challenges and limitations of MRI AD detection are discussed, along with strategies for achieving early detection. Insights into how machine learning and AI can enhance diagnostic accuracy are also provided [4]. Additionally, the importance of a multi-disciplinary approach, bringing together clinicians, neuroscientists, radiologists, and computer scientists, is emphasized to fully leverage the potential of MRI for early Alzheimer's diagnosis. By examining the state-of-the-art in MRI AD detection and looking ahead to future developments, this work aims to contribute to the fight against Alzheimer's and improve quality of life [5].

Recent developments in medical science have revealed that Alzheimer's disease is the most widespread disease in the world. Early detection and treatment of this condition can be lifesaving. To address this, increased research initiatives have been conducted to identify high-quality patterns in large amounts of data.

The proposed algorithm includes the use of MRI scan images to detect Alzheimer's disease, as well as the implemented algorithm in four phases Adaptive Median Filtering-Based Pre-processing (AMFP) is the first step in the preprocessing of MRI scanned images. Discrete local binary pattern (DLBP) and a hybrid wavelet partial Hadamard transform (Hybrid WPHT) are then used to extract features from the preprocessed image. Next, the Harris-Hawk adaptive optimization (AHHO) approach is used to reduce feature dimensionality. Lastly, the Improved Weight-Based Bug Swarm (IW-BS) algorithm is used to adjust the parameters of the SVM approach to improve classification performance.

The structure of this paper is as follows: Section 2 review recent related publications, the proposed method is elaborated upon in Section 3, the results and discussions are described in Section 4, and the research is summarized in Section 5.

The advancement of neuroimaging technology, which has enabled healthcare providers and researchers to acquire many neuroimaging datasets, is one of the emerging technologies that are beneficial to healthcare providers. Several sophisticated algorithms have been developed to identify AD. This document lists the several algorithms that have been created to identify Alzheimer's disease, classifying them into two groups: deep learning-based methods and classical machine learning-based methods.

The use of machine learning algorithms has been incorporated into the innovations, resulting in a marked acceleration in the diagnosis and management of Alzheimer's. The researchers have employed established pattern analysis techniques. To develop prediction models for the early diagnosis of Alzheimer's disease, logistic regression (LR), support vector machines (SVM), and linear discrimination analysis (LDA) are used [6]. The primary impediment to utilizing these outdated categorization techniques is the duration required to complete these stages, as they necessitate expertise and a multitude of stages of refinement [7].

Beheshti et al. [8] this study utilized structural magnetic resonance imaging (MRI) scans from Alzheimer's Disease Neuroimaging Initiative (ADNI) database for 130 individuals with Alzheimer's disease and 130 individuals with non-Alzheimer's disease. Each participant was given neuropsychological tests to acquire clinical indicators, such as results from the Clinical Dementia Ratio and the Mini-Mental State Examination. Additionally, the study employed a feature ranking based on the reduction of classification error and Voxel-based feature extraction technique. The proposed model was found to be accurate with a 92.48% accuracy rate. In a separate study, Zhang et al. [9] This study conducted a comprehensive analysis of longitudinal MRI scans from ADNI database, which included data from 207 healthy subjects and 154 patients with Alzheimer's disease. The data-driven approach to landmark discovery was employed to identify landmarks, and a landmark based feature extraction framework was proposed to extract statistical, that used a bag-of-words technique to extract statistical high-level spatial and contextual longitudinal information. Based on the results of the study, the SVM classifier was employed, achieving an impressive 88.30% accuracy rate. In a study conducted by Zeng et al., [10] using the ADNI database of MRI scans from 82 patients with normal control (NC) and 92 Alzheimer's Disease (Alzheimer's), Voxel features were extracted using an automated anatomical labeling template, a hybrid model was proposed by employed the switching delayed particle swarm's optimization technique and principal component analysis to optimize the kernel parameter and the penalty factor of SVM classifier. According to the outcome, the proposed classifier with accuracy level of 71.23%. In a recent study conducted by Koh et al. [11] using MRI brain scans from Harvard Brain Atlas and UMAC databases, 55 Alzheimer's patients and 110 healthy subjects were scanned. Subsequently, features were extracted using the Bidirectional Empirical Mode Decomposition technique. The results indicated that RF classifiers and a single-degree polynomial kernel (SVM) reached 93.9% accuracy. The primary obstacle to the implementation of standard machine learning lies in the requirement to extract features from a wide range of neuroimaging images and feed them into classification algorithms.

Deep learning (DL) is a rapidly developing area of machine learning that utilizes raw neuroimaging information to generate characteristics through "on-the-go" learning, and is becoming a major topic of research in large-scale, highly dimensional neuroimaging analysis [12].

In Liu et al., [13] a deep learning model for Alzheimer's disease diagnosis was developed through research. Fluorodeoxyglucose-positron emission tomography (DFDG-PET) neuroimaging served as the foundation for this concept. 2D slices were created from 3D FDG-PET pictures. The slices were then sorted into nine categories according to how similar their structural features were. Features were extracted using deep learning approaches, such as a 2-stacked bidirectional-gated recurrent unit cascaded to extract inter-slice features and a 2D CNN model trained for intra-slice extraction. The final classification output was fed into two fully connected layers and a SoftMax layer. The results of the study test on 100 healthy participants and 93 patients with AD from the ADNI database. It showed that the proposed model was accurate to 91.2%.

P. Vemuri, [14] used 3D-MRI images from ADNI database, which included 139 healthy subjects and 198 patients with AD. The tissue image was composed of three types. Cerebral spinal fluid (CSF), white matter (WM), and gray matter (GM). These tissues were subjected to parallel 3D Multi-Scale-CNNs, which enabled the extraction of multispectral features. Furthermore, two separate fusion layers were performed on different scales of the tissue region and adjacent tissue regions.

The results of the study by Basia et al. [15], 124 individuals with Alzheimer's disease and 50 normal participants' MRI scans were acquired using the Milan database. It was discovered that the suggested model, which consists of twelve convolutional layers with LR output layer and fully connected layer with ReLU activation function and repeated blocks, was extremely accurate (98 percent) for both data sets.

Pan et al. [16] used 3D- MRI scan image of 162 healthy subjects and 137 AD subjects from ADNI database to construct a model. The model was designed to extract features from a collection of coronally, sagittalally, and transversally scanned 2D-MRI slices. Subsequently, the extracted features were combined with multiple 2 D-CNN models to construct a specialized ensemble model that yielded the classification result. The model has demonstrated successful performance with an 84% based on 10-fold Cross-validation of the data set.

In addition to Feng et al. [17] used ADNI database 3D MRI images for 159 healthy individuals and 153 Alzheimer's disease patients. Three models were presented, namely 2D-CNN, 3D-CNN, 3D-CNN-SVM to extract features from scans, and SVM to perform classification tasks based on the extracted features, and the most successful model according to their experimental findings 99.10% accuracy, 99.40% specificity, and 98.80% sensitivity.

Li et al. [18] conducted a study in which 174 healthy subjects and 116 patients having Alzheimer's disease were enrolled in the study. The participants were scanned with 4D-MRI scans from the ADNI database. The proposed model was constructed using a combination of two different approaches: 3D-CNN used to extract features from scans, and Long-Term Memory-Based (LSTM) classification of derived features. 3D CNN could capture spatial information, while LSTM

enabled the capture of time-varying features. According to the experiments conducted, the model achieved a high level of performance, with 95.37% accuracy.

In a recent study conducted by Liu et al., [18] used OASIS database from 30 AD patients and 332 healthy subjects. Resampling techniques were applied to the dataset, resulting in a last version with 450 Alzheimer's patient scans and 532 average healthy subjects. Additionally, the model was tested with a few ADNI database. The proposed model, which differs from the default CNN by dividing the convolution layer into filtering layers and feature extractors, is a depth-wise separable CNN.

In addition to GoogNet and AlexNet[1], the fundamental CNN paradigm was also employed through transfer learning. The results of the tests indicated that transfer learning yielded to accuracy level for GoogleNet, at 93.02%. Previous studies have demonstrated that deep learning methods, which do not necessitate a feature extraction phase, are more precise and effective than traditional machine learning techniques. Furthermore, the accuracy and efficiency of the results are enhanced due to the high number of images used in Alzheimer's neuroimaging kinds. Nevertheless, there is still potential for further refining deep learning methods for the management of neuroimaging datasets, particularly datasets with multiple frames per patient, each with a distinct set of properties; all frames are coupled and display significant changes [19–21].

2. MATERIAL AND METHODS

To reduce the dimensionality of feature selection, this paper aims to develop a framework for the diagnosis of AD using MRI images processed through Adaptive Median Filtering-Based Hybrid Wavelet Partial Hadamard Transform (Hybrid-WPHT) combined with Discrete Local Binary Pattern (DLBP), an Adaptive Harris Hawk Optimization Strategy sub-process. This study employed OSVM for classification and an enhanced Weight-Based Beetle Swarm (IW-BS) Algorithm for parameter tweaking. The suggested framework for detecting Alzheimer's disease is shown in Figure 1.

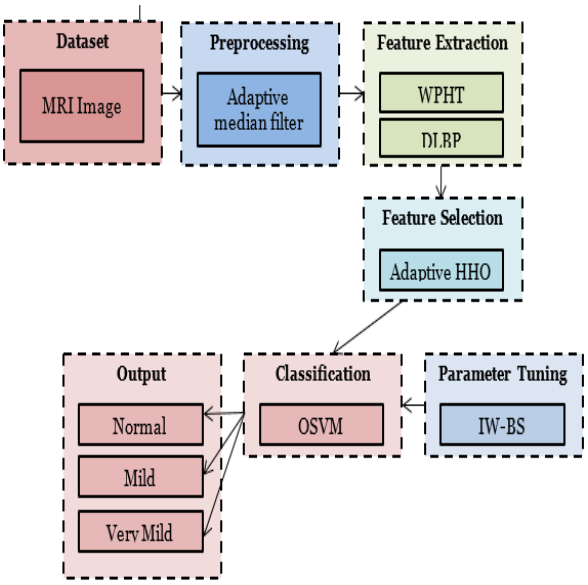

Fig. 1. The proposed technique Alzheimer's disease detection.

2.1. Pre-processing

In order to detect and eliminate noisy pixels in MRI images, an **adaptive median filter (AMF)** is employed [22,23]. When positioned over an MRI, the pixels in the p × p window are arranged in ascending order. The minimum and maximum pixel values are determined in p×p window. Next, determine if any value is the same as the center pixel, then the center pixel is considered a noisy pixel. The window should cover the middle pixel, and it should be centered by selecting an odd number for p.

In the p × p window, the number of neighboring pixels is also shown by the symbol m. The filtered value is given by the following equation.

$$F_{Value} = M\,[P_j^{(m-1)}\ ;\ j\epsilon\, P] \quad (1)$$

Where p × p sub-window, m stands for the total number of surrounding pixels and j for the number of pixels that surround the center pixel. The pixels in the p × p sub window and their surrounding pixels are listed in the following equations.

$$P_j^{(m)} = \begin{Bmatrix} n_j^{(m-1)} & |\ if\ h_j^{(m-1)} == 1, \\ p_j^{(m-1)} & else \end{Bmatrix} \quad (2)$$

$$h_j^{(m)} = \begin{Bmatrix} h_j^{(m-1)} & |\ if\ p_j^{(m)} = p_j^{(m-1)}, \\ 0 & else \end{Bmatrix} \quad (3)$$

The remaining pixels are then organized in ascending order after the minimum and maximum values in the p × p window are removed. In the Alzheimer's MRI image, the noisy pixel value is utilized instead of the center pixel value.[24].

2.2. Feature Extraction

After image pre-processing, the features are extracted from the MRI images Using DLBP model and Hybrid-WPHT.

2.2.1. Discrete Local Binary Pattern model

For some photos that employ the grey level for every pixel, the LBP function offers the descriptor [25,26]. In the default implementation, a pixel is considered to have eight neighbors, resulting in the square of 3 × 3 pixels. LBP function is as follows:

$$LBP(x_c, y_c) = \sum_{p\epsilon P} 2^p * q(i_q - i_c) \quad (4)$$

Where P is the framework that describes the dominating pixels nearby pixels i_c and i_p are the center pixels and their p^{th} neighbor's respective grey levels, and q (z) is the quantization function [25].

The latest version of the LBP is focused on finding an optimal threshold that will distribute all the pixels within a patch. Once these thresholds are achieved, the following minimum remaining error is calculated.

$$\varepsilon(t) = \frac{1}{N}\{\sum_{i|I(r_i)\le t}(I(r_i) - \mu_o)^2 + \sum_{i|I(r_i)\le t}(I(r_i) - \mu_1)^2 \quad (5)$$

With:

$$\mu_0 = \frac{1}{N_0}\sum_{iII(r_i)\le r} I(r_i) and\ N_0 = \sum_i q\big(t - I(r_i)\big) \quad (6)$$

$$\mu_0 = \frac{1}{N_1}\sum_{iII(r_i)\le r} I(r_i) and\ N_1 = \sum_i q(I(r_i) - t) \quad (7)$$

The intra-class variance 2 w was previously designed as the remaining error (z). Following the determination of the threshold, it can be predicted that the weight of all pixels spliced together on the preceding histogram will be:

$$\omega = \sqrt{\frac{\sigma_B^2(\gamma^*)}{\sigma^2+C}} \quad (8)$$

Where C denotes a constant that is used to handle specific instances where 2 is close to zero and can cause the vote weights to vary, and 2 can be found at 0.012. With (radius, neighbors) = (1, 8), (2, 8), this feature is gone (3, 8).

2.2.2. Partial Hadamard transform based on wavelets

DWT and PHT (a Partial Hadamard transform) were used to produce feature extraction results that were more effective [25,26]. These derived features have three main applications: translation, rotation, and scaling. The partial Hadamard transformation was used to recover the parameters of the multidirectional low frequency sub bands after the segments had been processed using a 2-level DWT. This illustrates how low-pass and high-pass filters can be applied progressively to a segmented image using DWT to retrieve its attributes. The following equations illustrate the procedure for obtaining a feature using a wavelet based partial Hadamard transform.

$$g(y) = \sum_l b_{j0}(l)\varphi_{f_j(y)} + \sum_{j==j_0}^{\infty}\sum_l C_j(l)\omega_{j,l}(y) \quad (9)$$

Where C_j and b_{j0} stand for the approximate expanded coefficient for the coarser signal and the wavelet coefficients. The fundamental functions $j_{0,l(y)}$ and $j_{,l(y)}$, respectively, are produced by the translation and dyadic dilation process.

$$\Psi_{j0,1}(y) = 2^{\frac{j}{2}} f_j\left(2^j y - l\right) \quad (10)$$

$$\Psi_{j,1}(y) = 2^{\frac{j}{2}} h_j\left(2^j y - l\right) \quad (11)$$

As a result, the translation and dilation parameters and the high pass and low-pass filter coefficients are represented for the liver tumor picture as l. Both fi and hi are used to refer to it. The partial Hadamard transform is explained using the following steps. A row vector of length n is represented by the notation B = [b1, b2,.....bn]. Equation 2 shows how to conduct the partial Hadamard transform once q has been produced using the random vector B. (12),

$$y_h = q_x y_D \quad (12)$$

By meeting the requirements for a Hadamard transform, the complex value vector y_h is created. A Hadamard matrix's transformations are irreversible, and its row-reduced sub matrix, q_x, is always column-rank deficient. The DWT Partial Hadamard Transform provides a function with a value range of +1 to -1. The partial Hadamard transformation is less computationally difficult and can be carried out utilizing numerous Hadamard transform constructions; equation (12) did not include a multiplication operation. The feature vectors for every segment are calculated using the Partial Hybrid Hadamard transform. To identify the related segments, the attributes of each segment must be compared after recovery.

2.3. Feature selection

In reaction to the Harris Hawk's hunting technique, which is often referred to as "the seven kills" or "the "unexpected" pounce," the Adaptive Harris Hawk Optimization (AHHO) meta-heuristic algorithm was created.[6,27]. There are two crucial steps in the HHO modeling process (exploitation and exploration). The first theory states that Harris hawks would take up residence anywhere that was within close range of group homes. Prey will function as features, and hawks as searchers. [29]. Depending on the fitness function, the best features are chosen to use the AHHO method. The formula for computing a fitness function is:

$$fitness\ function = \alpha * \boldsymbol{\xi} + (\mathbf{1}-\boldsymbol{\alpha}) * \frac{\boldsymbol{IM_e I}}{\boldsymbol{IM_d I}} \quad (\mathbf{13})$$

The error value presented in a classification is written as follows: Me is the total number of features extracted from the feature extraction stage, Md is the total number of features in the dataset that was provided and indicates the parameter impacting the outcome of a classification step. The way in which equation (14) represents this condition is explained below.

$$\begin{cases} Y_{ran}(s) - r_1|Y_{ran}(s) - 2r_2Y(s)|, & q \geq 0.5 \\ \left(Y_{features}(s) - Y_n\right) - r_3\left(LV + r_4(UV)\right), & q \geq 0.5 \end{cases} \quad (14)$$

The search agent's location vector, Y (s+1), is represented by Y (s), the most recent position vector of the search agent, Y_{ran} (s), a randomly chosen search agent from the current population, and r_1, r_2, r_3, r_4, and p are random numbers of (0,1). The position of the features is indicated by $Y_{features}$ (s), where UB is the bottom variable and LV is the upper variable. The average location of the search agent population currently is Y_n.

It is suggested that the search agent returns to the place of a feature or $Y_{features}$ if it crosses the permitted boundaries, which is the optimal course of action as follows:

$$Y(s+1)\begin{cases} Y(s+1), & Y_{min} \leq Y(s+1) \leq Y_{max} \\ Y_{features}(s), & Y(s+1) < Y_{\min} \\ Y_{features}(s), & Y(s+1) > Y_{\max} \end{cases} \quad (15)$$

An AHHO-based feature selection approach optimizes the selection of the features, thereby reducing the computational complexity of the classification process.

2.4. Detecting Alzheimer's illness with optimum SVM

The best SVM [30] successfully detects and categorizes Alzheimer's disease from other diseases in MRI scan pictures. The global optimized and maximum generalized capabilities of SVM are a significant advantage. SVM has the advantage of being globally optimized and having the highest possible generalized capabilities. In addition, compared to existing techniques, it solves the over fitting issues and provides sparse solutions. The standard linear classifier problems, namely 1, 2e, are distinguished from the trained data set, (x_i, y_i); I = 1, 2, 3,..., m. Here, m is the number of observations made available, xi Rn denotes feature vectors, and $y_{i\ (-\ 1,\ +1)}$ denotes label vectors. The binary classifier problem is described as an optimal problem as follows:

$$Min: \frac{1}{2}||w||_2^2 + C\sum_{i=1}^{m}\xi_i \quad (16)$$

$$subjected\ to:$$

$$y_i(w \times x_i) + b \geq 1 - \boldsymbol{\xi_i}, \boldsymbol{\xi_i} \geq \mathbf{0}, \boldsymbol{i} = \mathbf{1}, .. \boldsymbol{m} \quad (\mathbf{17})$$

If I is the variable that describes the penalizing relaxation, C stands for the regularization parameters, and equation (18) is:

$$w \times \left(\varphi(x_i)\right) + b \geq +1\ if\ y_i = +1 \quad (18)$$

$$w \times \left(\varphi(x_i)\right) + b \geq -1\ if\ y_i = -1 \quad (19)$$

The non-linear classification could be signified in the input space as:

$$f(x) = sign\left(\sum_{i=1}^{m} \alpha_{j*} \times y_i \times K(x_i, y_i\right) + b^*) \quad (20)$$

where f (x) is the decision function and the bias b* has been determined using the Karush-Kuhn-Tucker (KKT) condition. The inner product is transported to this feature space by the kernel function, represented by K (x_i, y_i). The following radial basis function (RBF) is used in this case:

$$K(,y) = \exp(-\gamma||x - y||^2) \quad (21)$$

wherein the indicated kernel parameters were found. For increased efficiency, a few SVM parameters require that the regularized parameter C and the kernel parameter be included in the elect property.

When the value of parameter C is excessively high during both the training and testing phases, the accuracy of the classification is exceptionally high during the training phase but severely low during the testing phase. The classification has an inadequate accuracy rate when the value of C is too low, making the model useless. The value of the parameter has a significantly higher effect on the classification result compared to the value of the C parameter, as its value influences the partitioning of the feature space. Consequently, the over-fitting or under-fitting of the parameter is due to the immense value of the parameter and the small value of the parameter, respectively. The BSA technique can be used to improve the correct selection of parameters values. The maximum classification accuracy can be achieved by the classifier if the error rate of the classifier is kept at a minimum. The SVM model for classifying the data is provided in Figure 2.

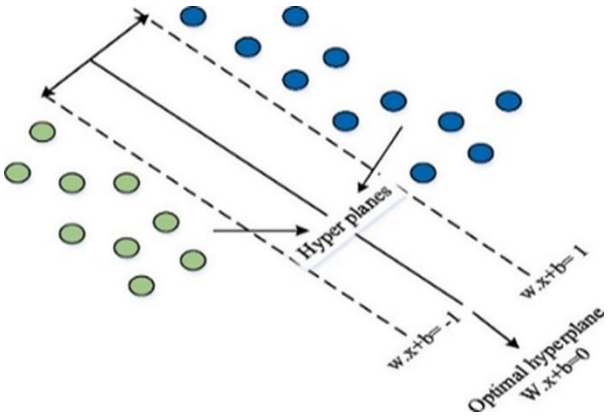

Fig. 2. Alzheimer's disease detection proposed SVM hyperplane.

2.4.1. Optimizing parameters with an enhanced weight-based beetle swarm algorithm

The Insect Swarm System is an innovative intelligent algorithm based on the concepts of beetle foraging, which has been successfully adapted to the SVM method [31]. The Beetle Swarm (BS) algorithm is based on the beetle's search engine and prey parameters [30], which are suitable for SVM classification. The formula for computing the fitness function is as follows:

Fitness function = max*imization* (*accuracy*) (22)

During the SVM parameter search, the antenna's orientation is transformed into a random vector, where rand is a random function, and l is the size of the optimization problem.

$$\underset{c}{\rightarrow} = \frac{rand\ (l,1)}{\|rand\ (l,1)\|} \quad (23)$$

The left and right antennae's spatial coordinates are determined as:

$$\begin{cases} y_{si} = y^i \\ y_{ki} = y^i + b^{*\rightarrow}c/2 \end{cases} + \frac{b^{*\rightarrow}c}{2} \quad (i = 1,2ldotsn) \quad (24)$$

where b indicates the distance between the two antennae, y_i indicates the centroid coordinate between the two antennae at the i^{th} iteration, and y_{si} and y_{ki} indicate the position coordinates of a left and a right antenna, respectively, at the i^{th} iteration. Utilizing the objective function, determine the values for the left and right antennas, then use the following formula to update the search agent's position.

Calculating antenna values of the left and right using the goal function and updating the search agent's position using the formula provided below.

$$y^{i+1} = y^i - \delta^{i*} \underset{c}{\rightarrow} * sign\big(f(y_{st}) - f(y_{ki})\big) \quad (25)$$

where sign() is a sign function, and I is a step factor at the i^{th} iteration. The step factor is one important component that influences the BAS algorithm's search capabilities. By doing this, the algorithm is released from having to choose local best solutions and can explore the whole search space. A step factor's value progressively decreases with an increase in iterations, improving the algorithm's ability to exploit local conditions. The inertia weight value is used in this work to improve bug swarm optimization. Lower weight can increase the search agent's capability for local searching in later phases, while higher values can speed up the search agent for new locations. Here are the updated equations:

$$w = w_{min} + \frac{(w_{max} - w_{min})(i_{max} - i)}{i_{max}} \quad (26)$$

$$y^{i+1} + wy^i - \delta^{i*} \underset{c}{\rightarrow} * sign\big(f(y_{si}) - f(y_{ki})\big) \quad (27)$$

Where i_{max} number of iterations is the maximum, w_{max} is the maximum and w_{min} is the minimum criteria for the inertia weight. Each classifier for each dataset is trained with a 70% training data, and the performance of the classifier is evaluated by correctly classifying a 30% sample of test samples. Metrics including accuracy, specificity, recall, precision, F-score, running time, AUC, and ROC are used to gauge performance.

Accuracy: This is the percentage of correctly predicted data from the network divided by the total amount of data.

$$A_c = \frac{t_p + t_n}{t_p + f_p + f_n + t_n} \quad (28)$$

(False Negative: True Negative; True Positive: False Positive; True Negative: False Positive).

Specificity: The quantity of data appropriately regarded as negative out of all negative data is given in the equation below (29),

$$S_{pe} = \frac{t_n}{f_t + t_n} \quad (29)$$

Recall: is defined as the proportion of positive data that were correctly identified divided by the total amount of such data. The following formula is as follows:

$$R_{ecall} = \frac{t_n}{f_n + t_p} \quad (30)$$

***Precision**:* measures a model's capacity for t_p detection and is calculated under the equation (31).

$$P_{rec} = \frac{t_p}{f_p + t_p} \quad (31)$$

F-Score: The F1 score is a measure of a model's overall accuracy that strikes a favorable balance between recall and precision. It is determined using equation (32),

$$f_{score} = 2 \times \frac{P_{rec} \times R_{ecall}}{P_{rec} + R_{ecall}} \quad (32)$$

Running time: is a measure of the time required to execute a computer program. One way to think of a computation is as a series of rule applications, where the number of applications is inversely related to the calculation time.

AUC: A parameter is used to analyze network performance and classify data into the appropriate categories. A value of 1 indicates complete categorization, while a value of 0 indicates a definitive classification failure. The ROC parameter was also used to investigate the AUC.

ROC: This is a graph that shows how classification models perform across all levels of categorization. Absolute Positive Rate and Inaccuracy Positive Rate are its two constituent parameters.

3. RESULTS AND DISCUSSION

The experimental outcomes of the suggested WPHT-OSVM Alzheimer's disease detection approach are reviewed in this section. Other modern approaches are also examined to see how effective the suggested approach is. MATLAB is used to implement the suggested method, and memory recall, specificity F-score, precision, run-time, precision, area under the curve (AUC), and receiver operating characteristic are used to assess the method's effectiveness (ROC).

3.1. Datasets

Two datasets, Benchmark Alzheimer's database [32] and ADNI [33], are used to diagnose Alzheimer's disease. Benchmark Alzheimer's database consists of 300 MRI Scan, which are three class labels: normal, mild demented and very mild demented. Each class contains 100 photographs.

Table 1: Performance comparison of the proposed technique and other algorithms across multiple evaluation metrics, including precision, accuracy, recall, specificity, F-score, AUC, and running time (in seconds), on two datasets.

algorithm	precision	Accuracy	Recall	specificity	F-Score	AUC	running time (sec)
proposed technique on dataset 1	99.24	99.35	99.28	99.47	99.27	98.57	1.26
proposed technique on dataset 2	99.33	99.55	99.33	99.66	99.33	99.8	1.01
ANN	94.95	97.13	95.66	96.24	96.3	83.4	9.42
CNN	96.85	97.85	95.19	96.56	95.59	83.99	8.15
ResNet50	97.61	96.22	96.64	96.49	96.51	80.8	7.53
AlexNet	97.36	95.38	97.28	95.73	95.52	9.57	5.61
VGG16	95.23	97.95	96.42	97.01	97.18	87.87	3.18

ADNI consists of 1018 Institute Alzheimer's MRI scans, together with Proteomics and Genetic Experiment data. All eligible radiographs are classified as either normal or demented in this paper.

This study utilized two datasets—Benchmark Alzheimer's database and ADNI—each containing varying degrees of Alzheimer's severity. The proposed method consistently outperformed existing techniques in terms of accuracy, recall, specificity, and runtime efficiency. However, the inclusion of additional datasets with varying imaging modalities, resolutions, and patient demographics could further validate the approach.

As a future direction, the evaluation will be expanded to include datasets with diverse characteristics and the method will be tested under different imaging scenarios, such as varying levels of noise and distortions. This would not only enhance the generalizability of the findings but also ensure the method's applicability in real-world clinical settings.

3.2. Performance analysis

The performance evaluation's findings show that, in terms of accuracy, recall, F-score, specificity, running time, AUC, and ROC, the suggested method outperforms the competition when compared to current approaches.

To analyze the given table scientifically, it is necessary to focus on the performance metrics across different algorithms, including the proposed technique, and consider their strengths and weaknesses in various aspects. A breakdown of the key metrics is provided below:

1. Precision:
Precision measures the proportion of positive results that were correctly identified (True Positives / (True Positives + False Positives)).

Proposed technique on Dataset 2 shows the highest precision at **99.33%**, followed closely by **Proposed technique on Dataset 1** at **99.24%**. This suggests that the proposed technique is highly accurate in identifying positive instances.

The **ANN** and **CNN** models, while good, show lower precision compared to the proposed technique (**94.95%** and **96.85%**, respectively).

2. Accuracy:
Accuracy represents the proportion of total correct predictions (True Positives + True Negatives) out of all predictions.

The **Proposed technique on Dataset 2** achieves the highest accuracy at **99.55%**, followed by **Proposed technique on Dataset 1** at **99.35%**. This indicates that the proposed technique performs extremely well in overall classification.

Other algorithms like ANN **(97.13%)**, **CNN (97.85%)**, and **ResNet50 (96.22%)** have lower accuracy, but they still perform quite well.

3. Recall:
Recall (also known as Sensitivity or True Positive Rate) measures the proportion of actual positive instances that are correctly identified.

Proposed technique on Dataset 1 has **99.28%** recall, with **Proposed technique on Dataset 2** achieving **99.33%**, which is slightly better. This shows that the proposed technique excels at identifying most positive instances.

The **ANN** model shows **95.66%** recall, indicating that some positive instances are missed. The **CNN** and **ResNet50** models also show lower recall than the proposed technique, although they still perform adequately.

4. Specificity:
Specificity (also known as True Negative Rate) is the proportion of actual negative instances that are correctly identified.

The **Proposed technique on Dataset 2** has the highest specificity at **99.66%**, followed closely by the **Proposed technique on Dataset 1** at **99.47%**.

ANN (96.24%), **CNN (96.56%)**, and **VGG16 (97.01%)** are somewhat lower in specificity, suggesting that they misclassify more negative instances compared to the proposed technique.

5. F-Score:
The F-score (or F1-score) is the harmonic mean of precision and recall, providing a balanced measure of performance for both metrics.

Both proposed techniques (Dataset 1 and 2) lead in F-score with **99.27%** and **99.33%**, respectively, indicating excellent performance in balancing precision and recall.

ANN (96.3%), **CNN (95.59%)**, and **ResNet50 (96.51%)** have a noticeably lower F-score, implying some trade-off between precision and recall.

6. AUC (Area Under the Curve):
AUC measures the ability of the model to distinguish between positive and negative classes. A higher AUC indicates better overall performance.

Proposed technique on Dataset 2 achieves the highest AUC at **99.8%**, followed by **Proposed technique on Dataset 1** at **98.57%**, indicating that the proposed method has an excellent ability to discriminate between classes.

The **ANN (83.4%)**, **CNN (83.99%)**, and **ResNet50 (80.8%)** models perform considerably worse in terms of AUC.

7. Running Time (Seconds):
Running time measures the computational efficiency of the algorithm. The **Proposed technique on Dataset 2** has the shortest runtime at **1.01 seconds**, followed by **Proposed technique on Dataset 1** at **1.26 seconds**, making it highly efficient.

ANN (9.42 seconds), **CNN (8.15 seconds)**, and **ResNet50 (7.53 seconds)** have much longer running times, suggesting they are less efficient compared to the proposed technique.

AlexNet (5.61 seconds) and **VGG16 (3.18 seconds)** show intermediate performance in terms of efficiency, but still, the proposed technique is significantly faster.

The proposed technique shows superior performance across all metrics (precision, accuracy, recall, specificity, F-score, AUC), making it highly effective in terms of both performance and efficiency. It also has the shortest running time, which is a significant advantage in practical applications. While **ANN**, **CNN**, **ResNet50**, **AlexNet**, and **VGG16** perform well in several metrics, they generally lag the proposed technique in terms of precision, recall, AUC, and running time. Models like **ANN** and **CNN** show lower AUC and specificity, while **ResNet50** and **AlexNet** show lower recall and F-scores.

The accuracy of the suggested method is contrasted with the proven methods shown in Figure 3. The existing approaches, including optimal ANN, CNN, ResNet50, AlexNet, and VGG16, are evaluated with Dataset 1. Figure 4 compares the accuracy of the suggested technique applied to datasets 1 and 2 to that of other machine and deep learning techniques, achieving an accuracy of 99.35 percent on dataset 1 and 99.55 percent on dataset 2, respectively.

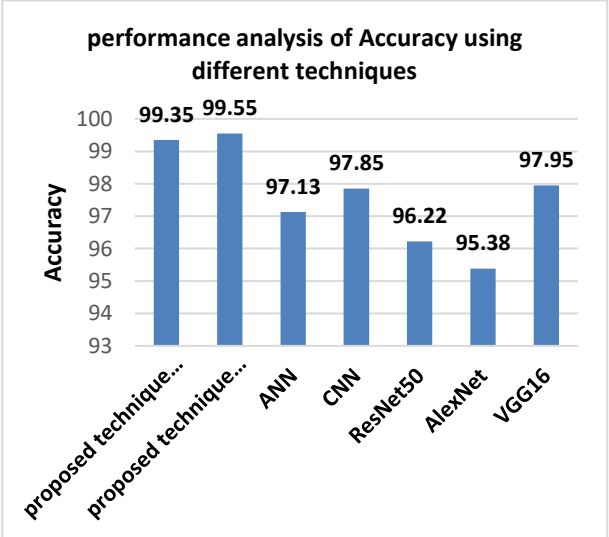

Fig. 3. Accuracy performance analysis utilizing various methodologies.

Figure 4 displays the findings of the precision performance research utilising both suggested and current approaches. With accuracy equal to 99.24 percent and 99.33 percent on datasets 1 and 2, respectively, Figure 5 compares the suggested technique applied to these datasets with other machine and deep learning techniques and achieves a greater precision.

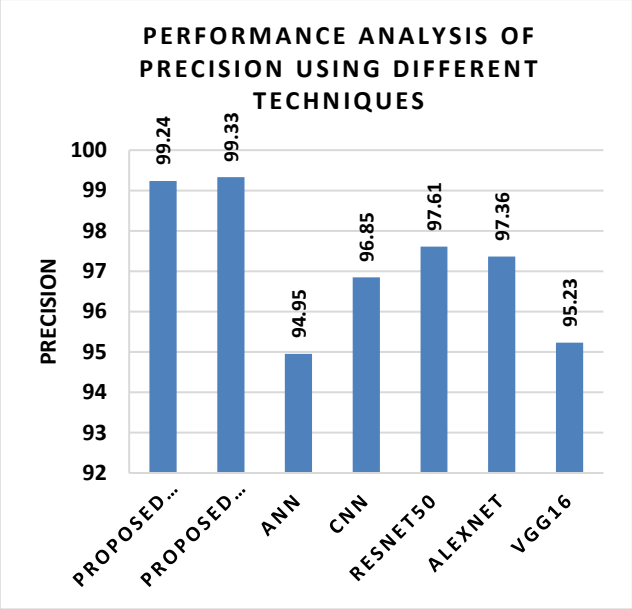

Fig. 4. Precision performance analysis using various methods.

The proposed method has demonstrated a positive recall performance compared to the existing approaches, as demonstrated in Figure 5. With accuracy equal to 99.28 percent and 99.33 percent on datasets 1 and 2, respectively, Figure 6 compares the suggested technique applied to these datasets to other machine and deep learning techniques and achieves a greater recall.

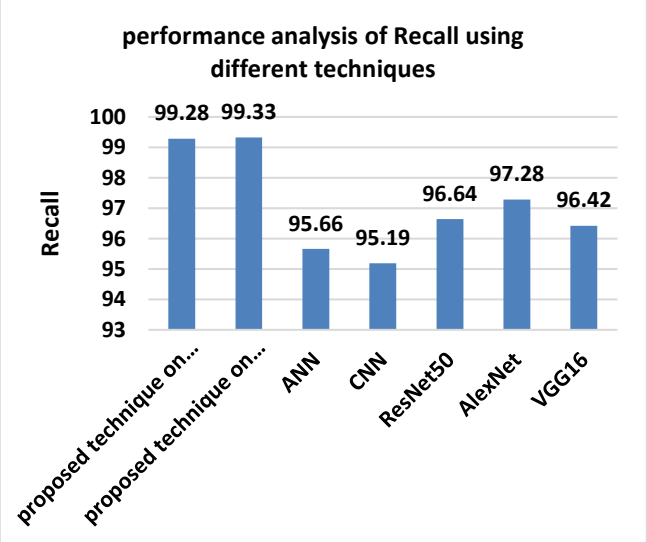

Fig. 5. Recall performance analysis utilizing various methods.

The specificity analysis of the suggested approach is contrasted with the existing methodologies in Figure 6. Figure 6 shows the comparison of the proposed technique applied upon datasets 1 and 2 have and achieve a higher specificity compared to other machine and deep learning techniques with accuracy equal to 99.47% and 99.66% on datasets 1 and 2, respectively.

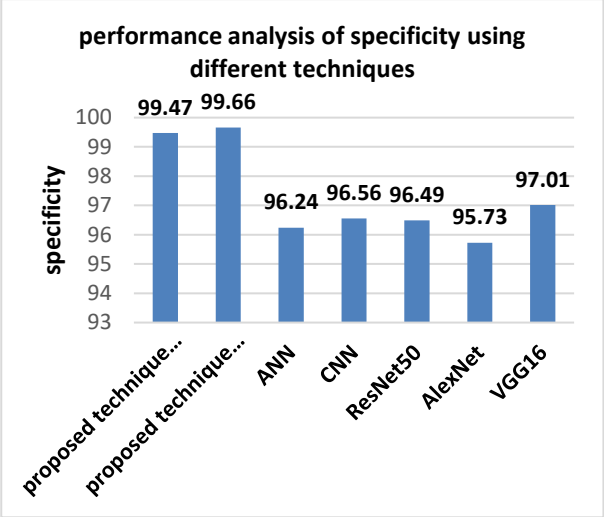

Fig. 6. Specificity performance analysis employing various methodologies.

In Figure 7, the proposed method's F-Score analysis is contrasted with the ones now in use. With an accuracy of 99.27 percent and 99.33 percent on datasets 1 and 2, respectively, the proposed technique on these datasets achieves a higher F-score in comparison to previous machine and deep learning techniques.

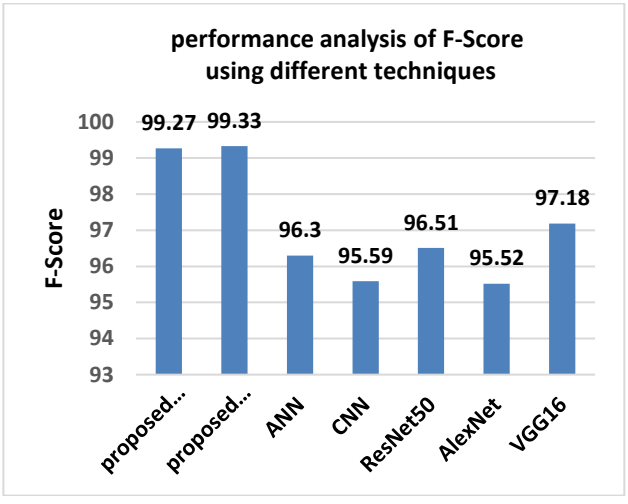

Fig. 7. F-score performance analysis utilizing various methods.

Figure 8 compares the running times of the present methodologies and a proposed approach. Figure 8 shows the comparison of the proposed technique applied upon datasets 1 and 2 have and achieve a higher accuracy compared to other machine and deep learning techniques with accuracy equal to 1.26 and 1.01on dataset 1 and 2, respectively. The proposed datasets 1 and 2 for the run-time performance are too low

compared to the existing techniques since the suggested study combines SVM with beetle Swarm optimization, which has a lower run-time performance, a faster global optimal solution, and reduced design complexity.

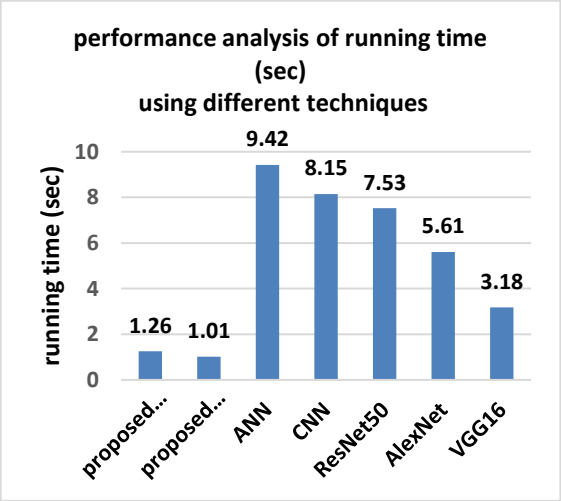

Fig. 8. Analyzing running time performance with various methods.

Figure 9 shows an AUC curve's performance analysis. Figure 9 shows the comparison of the proposed technique applied upon datasets 1 and 2 have and achieve a higher accuracy compared to other machine and deep learning techniques with accuracy equal to 1.26 and 1.01on dataset 1 and 2, respectively.

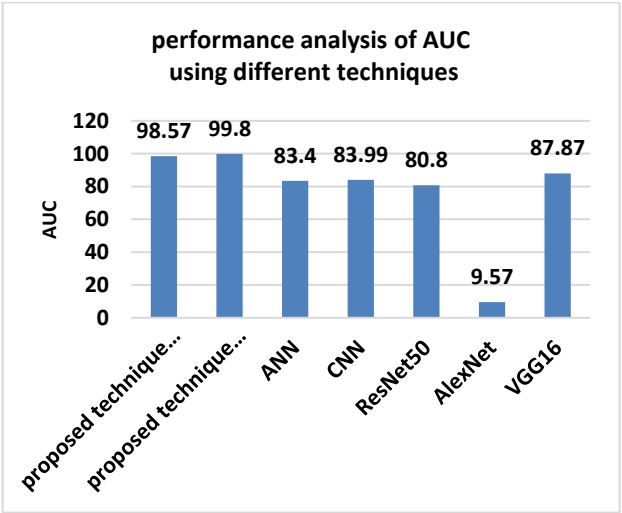

Fig. 9. Performance examination of AUC.

4. DISCUSSION

This work suggests an ideal Support Vector Machine (SVM) for Alzheimer's disease detection as well as a more effective weight-based optimization technique for beetle swarms. Zhang et al. [34] classify Alzheimer's disease diagnoses using an ensemble learning approach. and the accuracy is 98%. This approach is straightforward to comprehend and produces a higher accuracy than Zhang et al. algorithm [34]. However, the limitations of ensemble learning are more difficult to comprehend. The accuracy of Alzheimer's module classification with transfer learning in Raza et al. [35] is 94.21% and negative transfer is one of the major drawbacks of transfer learning. However, the proposed approach does not have these drawbacks and is more accurate than Raza et al. algorithm [35]. Furthermore, the SVM accuracy is 94% when using a deep learning-based model detection approach in Naji et al. algorithm [36].

An accuracy of 97.91 percent was achieved in the classification of medical images of Alzheimer's illness using the SVM based on Convolution neural network. However, the SVM has a number of drawbacks, including a longer training time, a higher number of features, and an excessive amount of noise. To overcome these limitations, researchers employed the optimization approach and an SVM classifier to categorize the Alzheimer's disease cell. The SVM classifier accuracy using CPSO (Chaos particle swarm optimization) in [37] was 97.4%, which identified the region and categorized the specific region using CPSO.

For the Kao et al. [38] algorithm, hybrid approaches based on Particle Swarm Optimization (PSO) and Genetic Algorithms (GA) based on Support Vector Machines (SVM) obtained 97.69 percent accuracy for Alzheimer's disease classification.. However, the drawbacks of PSO versus GA include a low convergence rate and a low convergence rate in computing complexity, among other factors. As SVM was combined with the beetle Swarm Optimization algorithm for the detection of Alzheimer's, the proposed method achieved an accuracy of over 98% in comparison to [35], [37], and [38]. The beetle Swarm has a simpler architecture, a more efficient global optimisation solution, and a shorter run time, allowing it to surpass the limitations of the SVM Classifier.

5. CONCLUSION

This study proposed the WPHT-OSVM framework for the precise detection of Alzheimer's disease using MRI images. The proposed method integrates advanced preprocessing, feature extraction, and classification techniques, achieving significant improvements in accuracy, precision, recall, and runtime compared to existing approaches. Performance evaluations demonstrated accuracy rates of 99.35% and 99.55% on two benchmark datasets, along with enhanced specificity and reduced computational complexity. These results indicate the effectiveness of the method for early and accurate detection of Alzheimer’s disease, providing a reliable diagnostic tool for healthcare professionals.

Future Scope

While the current study demonstrates promising outcomes, there is significant potential for further improvement. Future work will focus on validating the method on additional datasets featuring different imaging modalities (e.g., CT scans or PET scans), as well as larger and more diverse populations to ensure broader applicability. Additionally, integrating real-time clinical data and exploring its impact on performance will be considered. Extending the framework to include deep learning-based feature extraction and hybrid optimization algorithms could further enhance diagnostic precision. Moreover, the development of user-friendly, automated diagnostic systems based on this approach could facilitate deployment in clinical environments, particularly in resource-constrained settings. Finally, incorporating multi-modal data, such as genetic and proteomic information, could refine diagnostic accuracy and contribute to comprehensive patient profiling for personalized treatment planning.

Competing Interests

There was no specific grant from a public, private, or nonprofit funding organisation to sponsor this research. This manuscript was not aided in its drafting by any funding.

6. REFERENCES

[1] A.A.A. El-Latif, S.A. Chelloug, M. Alabdulhafith, M. Hammad, Accurate Detection of Alzheimer's Disease Using Lightweight Deep Learning Model on MRI Data, Diagnostics. 13 (2023) 1216. https://doi.org/10.3390/diagnostics13071216.

[2] J. Cummings, Y. Zhou, G. Lee, K. Zhong, J. Fonseca, F. Cheng, Alzheimer's disease drug development pipeline: 2023, Alzheimer's & Dementia: Translational Research & Clinical Interventions. 9 (2023) e12385. https://doi.org/10.1002/trc2.12385.

[3] W.M. van der Flier, M.E. de Vugt, E.M.A. Smets, M. Blom, C.E. Teunissen, Towards a future where Alzheimer's disease pathology is stopped before the onset of dementia, Nat Aging. 3 (2023) 494–505. https://doi.org/10.1038/s43587-023-00404-2.

[4] A.G. Vrahatis, K. Skolariki, M.G. Krokidis, K. Lazaros, T.P. Exarchos, P. Vlamos, Revolutionizing the Early Detection of Alzheimer's Disease through Non-Invasive Biomarkers: The Role of Artificial Intelligence and Deep Learning, Sensors (Basel). 23 (2023) 4184. https://doi.org/10.3390/s23094184.

[5] Researchers propose a novel biomarker for early diagnosis of Alzheimer's disease | Karolinska Institutet Nyheter, (n.d.). https://news.ki.se/researchers-propose-a-novel-biomarker-for-early-diagnosis-of-alzheimers-disease (accessed September 23, 2023).

[6] Y. Ding, J.H. Sohn, M.G. Kawczynski, H. Trivedi, R. Harnish, N.W. Jenkins, D. Lituiev, T.P. Copeland, M.S. Aboian, C. Mari Aparici, S.C. Behr, R.R. Flavell, S.-Y. Huang, K.A. Zalocusky, L. Nardo, Y. Seo, R.A. Hawkins, M. Hernandez Pampaloni, D. Hadley, B.L. Franc, A Deep Learning Model to Predict a Diagnosis of Alzheimer Disease by Using 18 F-FDG PET of the Brain, Radiology. 290 (2019) 456–464. https://doi.org/10.1148/radiol.2018180958.

[7] J. Samper-González, N. Burgos, S. Bottani, S. Fontanella, P. Lu, A. Marcoux, A. Routier, J. Guillon, M. Bacci, J. Wen, A. Bertrand, H. Bertin, M.-O. Habert, S. Durrleman, T. Evgeniou, O. Colliot, Reproducible evaluation of classification methods in Alzheimer's disease: Framework and application to MRI and PET data, NeuroImage. 183 (2018) 504–521. https://doi.org/10.1016/j.neuroimage.2018.08.042.

[8] I. Beheshti, H. Demirel, F. Farokhian, C. Yang, H. Matsuda, Structural MRI-based detection of Alzheimer's disease using feature ranking and classification error, Computer Methods and Programs in Biomedicine. 137 (2016) 177–193. https://doi.org/10.1016/j.cmpb.2016.09.019.

[9] Alzheimer's Disease Diagnosis Using Landmark-Based Features from Longitudinal Structural MR Images, (n.d.). https://ieeexplore.ieee.org/document/7929275/ (accessed September 24, 2023).

[10] N. Zeng, H. Qiu, Z. Wang, W. Liu, H. Zhang, Y. Li, A new switching-delayed-PSO-based optimized SVM algorithm for diagnosis of Alzheimer's disease, Neurocomputing. 320 (2018) 195–202. https://doi.org/10.1016/j.neucom.2018.09.001.

[11] J.E.W. Koh, V. Jahmunah, T.-H. Pham, S.L. Oh, E.J. Ciaccio, U.R. Acharya, C.H. Yeong, M.K.M. Fabell, K. Rahmat, A. Vijayananthan, N. Ramli, Automated detection of Alzheimer's disease using bi-directional empirical model decomposition, Pattern Recognition Letters. 135 (2020) 106–113. https://doi.org/10.1016/j.patrec.2020.03.014.

[12] JPM | Free Full-Text | Deep Learning-Based Diagnosis of Alzheimer’s Disease, (n.d.). https://www.mdpi.com/2075-4426/12/5/815 (accessed October 28, 2023).

[13] M. Liu, D. Cheng, W. Yan, Alzheimer's Disease Neuroimaging Initiative, Classification of Alzheimer's Disease by Combination of Convolutional and Recurrent Neural Networks Using FDG-PET Images, Frontiers in Neuroinformatics. 12 (2018). https://www.frontiersin.org/articles/10.3389/fninf.2018.00035 (accessed September 24, 2023).

[14] P. Vemuri, H.J. Wiste, S.D. Weigand, L.M. Shaw, J.Q. Trojanowski, M.W. Weiner, D.S. Knopman, R.C. Petersen, J. C R. Jack, O. behalf of the A.D.N. Initiative, MRI and CSF biomarkers in normal, MCI, and AD subjects: Predicting future clinical change, Neurology. 73 (2009) 294. https://doi.org/10.1212/WNL.0b013e3181af79fb.

[15] S. Basaia, F. Agosta, L. Wagner, E. Canu, G. Magnani, R. Santangelo, M. Filippi, Automated classification of Alzheimer's disease and mild cognitive impairment using a single MRI and deep neural networks, NeuroImage: Clinical. 21 (2019) 101645. https://doi.org/10.1016/j.nicl.2018.101645.

[16] D. Pan, A. Zeng, L. Jia, Y. Huang, T. Frizzell, X. Song, Early Detection of Alzheimer's Disease Using Magnetic Resonance Imaging: A Novel Approach Combining Convolutional Neural Networks and Ensemble Learning, Frontiers in Neuroscience. 14 (2020). https://www.frontiersin.org/articles/10.3389/fnins.2020.00259 (accessed September 24, 2023).

[17] Automated MRI-Based Deep Learning Model for Detection of Alzheimer's Disease Process | International Journal of Neural Systems, (n.d.). https://www.worldscientific.com/doi/abs/10.1142/S0129065720500320X (accessed September 24, 2023).

[18] J. Liu, M. Li, Y. Luo, S. Yang, W. Li, Y. Bi, Alzheimer's disease detection using depthwise separable convolutional neural networks, Computer Methods and Programs in Biomedicine. 203 (2021) 106032. https://doi.org/10.1016/j.cmpb.2021.106032.

[19] A. Wang, X. Yan, Z. Wei, ImagePy: an open-source, Python-based and platform-independent software package for bioimage analysis, Bioinformatics. 34 (2018) 3238–3240. https://doi.org/10.1093/bioinformatics/bty313.

[20] Data augmentation for improving deep learning in image classification problem, (n.d.). https://ieeexplore.ieee.org/document/8388338/ (accessed September 24, 2023).

[21] S. Indolia, A.K. Goswami, S.P. Mishra, P. Asopa, Conceptual Understanding of Convolutional Neural Network- A Deep Learning Approach, Procedia Computer Science. 132 (2018) 679–688. https://doi.org/10.1016/j.procs.2018.05.069.

[22] H. Soni, D. Sankhe, Student, Image Restoration using Adaptive Median Filtering, International Research Journal of Engineering IT & Scientific Research. (2019) 2395–0056.

[23] A. Shah, J.I. Bangash, A.W. Khan, I. Ahmed, A. Khan, A. Khan, A. Khan, Comparative analysis of median filter and its variants for removal of impulse noise from gray scale images, Journal of King Saud University - Computer and Information Sciences. 34 (2022) 505–

519. https://doi.org/10.1016/j.jksuci.2020.03.007.
[24] V. K, K. Kalaiselvi, Adaptive Median Filter Based Noise Removal Algorithm for Big Image Data, (2019). https://papers.ssrn.com/abstract=3318398 (accessed September 24, 2023).
[25] A Review of Local Binary Pattern Based texture feature extraction, (n.d.). https://ieeexplore.ieee.org/abstract/document/9596485/ (accessed September 24, 2023).
[26] S. Wang, G. Deng, J. Hu, A partial Hadamard transform approach to the design of cancelable fingerprint templates containing binary biometric representations, Pattern Recognition. 61 (2017) 447–458. https://doi.org/10.1016/j.patcog.2016.08.017.
[27] S. Song, P. Wang, A.A. Heidari, X. Zhao, H. Chen, Adaptive Harris hawks optimization with persistent trigonometric differences for photovoltaic model parameter extraction, Engineering Applications of Artificial Intelligence. 109 (2022) 104608. https://doi.org/10.1016/j.engappai.2021.104608.
[28] T. Zou, C. Wang, Adaptive Relative Reflection Harris Hawks Optimization for Global Optimization, Mathematics. 10 (2022) 1145. https://doi.org/10.3390/math10071145.
[29] A. Wunnava, M.K. Naik, R. Panda, B. Jena, A. Abraham, An adaptive Harris hawks optimization technique for two dimensional grey gradient based multilevel image thresholding, Applied Soft Computing. 95 (2020) 106526. https://doi.org/10.1016/j.asoc.2020.106526.
[30] Q. Wang, G. Cheng, P. Shao, An Adaptive Beetle Swarm Optimization Algorithm with Novel Opposition-Based Learning, Electronics. 11 (2022) 3905. https://doi.org/10.3390/electronics11233905.
[31] T. Wang, L. Yang, Q. Liu, Beetle swarm optimization algorithm: Theory and application, Filomat. 34 (2020) 5121–5137. https://doi.org/10.2298/FIL2015121W.
[32] Alzheimer MRI Preprocessed Dataset, (n.d.). https://www.kaggle.com/datasets/sachinkumar413/alzheimer-mri-dataset (accessed September 23, 2023).
[33] ADNI | Alzheimer's Disease Neuroimaging Initiative, (n.d.). https://adni.loni.usc.edu/ (accessed September 23, 2023).
[34] P. Zhang, S. Lin, J. Qiao, Y. Tu, Diagnosis of Alzheimer's Disease with Ensemble Learning Classifier and 3D Convolutional Neural Network, Sensors (Basel). 21 (2021) 7634. https://doi.org/10.3390/s21227634.
[35] Diagnostics | Free Full-Text | Alzheimer Disease Classification through Transfer Learning Approach, (n.d.). https://www.mdpi.com/2075-4418/13/4/801 (accessed September 24, 2023).
[36] Deep Learning Algorithm Based Support Vector Machines | SpringerLink, (n.d.). https://link.springer.com/chapter/10.1007/978-3-031-14054-9_27 (accessed September 24, 2023).
[37] Application of SVM Based on Improved Particle Swarm Optimization Algorithm in Epileptic Seizure Detection | IEEE Conference Publication | IEEE Xplore, (n.d.). https://ieeexplore.ieee.org/document/9549672 (accessed September 24, 2023).
[38] Y.-T. Kao, E. Zahara, A hybrid genetic algorithm and particle swarm optimization for multimodal functions, Applied Soft Computing. 8 (2008) 849–857. https://doi.org/10.1016/j.asoc.2007.07.002.